

SEDIMENT PROVENANCE OF THE BELT-PURCELL SUPERGROUP: IMPLICATIONS FOR THE MESOPROTEROZOIC SUPERCONTINENT COLUMBIA

Hirtz, Jaime A.¹

¹Jackson School of Geosciences, Department of Geological Sciences, University of Texas at
Austin, Austin, Texas 78712, USA

1. INTRODUCTION

The geologic record demonstrates our planet experienced drastic changes from cosmic bombardment to planetary differentiation, crustal formation, and continental drift amidst various climatic conditions. Perhaps the most intriguing of these is the concept of supercontinent cyclicality, characterized by the amalgamation and subsequent breakup of approximately 75% of the earth's landmass roughly once every 750 Myr. The existence of these ancient supercontinents is based on the observation of orogenic belts from the Phanerozoic (0.3-0.1 Ga), Neoproterozoic (1.1-0.9 Ga), Mesoproterozoic (2.1-1.8 Ga) and Neoproterozoic (2.8-2.6 Ga). Such interpretations have been supported by global zircon uranium-lead geochronological data where relative frequency probabilities show a temporal evolution that likely correspond to the waxing and waning of geologic activity associated with continental drift (Puetz, 2018). These arguments have been used to highlight the existence of paleo-supercontinents known as Pangea (McKenzie et al., 2015), Rodinia (Meert and Torsvik, 2003), Columbia (Meert and Santosh, 2017), and possibly Kenorland. However, back tracking the footsteps of nomadic cratons to piece together the crustal fragments of progressively older supercontinents is no easy feat. To first order, the tectonic configuration of

Pangea is relatively well constrained (McKenzie et al., 2015); however, paleotectonic reconstructions for Rodinia have higher margins of uncertainty, with postulations for Columbia and Kenorland being just that. For these reasons, numerous models for Columbia have been proposed that led to the longstanding debate over Laurentia's place within it all. Most arguments stem from ideas regarding the western margin of Laurentia during the Mesoproterozoic, with the only point-of-fact researchers seem to agree on being that a currently unknown craton collided, docked, rifted, and drifted away from modern day Idaho at ca. 1.5 Ga.

Based on current literature, most reconstructions for the western margin of Columbia fall into one of two camps. The first pertains to the Siberian hypothesis spearheaded by prominent scientists such as Raymond Price, James Sears, John MacLean, and John Lydon (Sears and Price, 2003; Lydon, 2007; MacLean and Sears, 2016), with the second being a combination of Antarctica and Australia led most notably by Gerald Ross among others (Ross and Parrish, 1991; Medig et al., 2014; Halpin et al., 2014; Jones et al., 2015). Proponents of the Siberian model typically place the Anabar shield directly adjacent to western Laurentia, while opponents have generally argued the Gawler and Terre Adélie craton of the Mawson continent (East Antarctica and South Australia) was directly west or southwest of Idaho. Both camps have touted articles with sensational titles such as the "Southwest U.S.-East Antarctic (SWEAT) connection" (Moore, 1991) and the "SWEAT and the end of SWEAT" (Piper, 2011), however, even in the age of modern technology, it appears both camps remain resolute.

Therefore, one of the best places on earth to gain some insight on this debate is the Belt-Purcell Supergroup of the northwest United States and southwest Canada. This is due to its geographic location along the western margin of paleo-Laurentia, proposed duration of deposition during the rifting of Columbia, and the fact that it contains arguably the best preserved sequences of

Mesoproterozoic rocks in North America. For these reasons, this study aims to narrow down the possibilities of supercontinent reconstructions by exploring isopach and paleocurrent data from Harrison (1972) and Cressman (1989). *To find any resolution, sediment source regions for the Belt-Purcell Basin must have a paleocurrent component originating from the mystery non-Laurentian craton situated to the west or south.*

2. DATA COLLECTION

2.1. State Boundaries

To begin testing this hypothesis, my methods involved collecting GIS data for state boundaries from the United States Geological Survey (table 1). I downloaded the FileGDB and unzipped the compressed folder in File Explorer. From there, the metadata within the decompressed file indicated the shapefile of interest is GU_StateOrTerritory and its spatial reference is the North American Datum of 1983.

2.2. Figures

Additionally, all figures containing necessary isopach and paleocurrent information were collected from Harrison (1972) and (Cressman, 1989). Formations are listed in stratigraphic order with oldest to youngest being bottom to top (table 1). I obtained this data by opening the .pdf of the published paper, found the figure of interest, took a screen capture, pasted it in the Paint program, cropped to the area of interest and saved each figure as a .tiff.

3. DATA PREPROCESSING

3.1. Projection

Since the spatial reference for the figures from Harrison (1972) and Cressman (1989) is unknown, I had to assume the authors used the North American Lambert Conformal Conic projection which is commonly used in the United States and Canada. Therefore, since the spatial reference of my shapefile for the US state boundaries was in NAD83, I needed to do a projection. This was accomplished by opening a blank map in ArcMaps and using ArcToolbox > Data Management Tools > Projections and Transformations > Project. I set the Input Dataset to GU_StateOrTerritory and changed the Coordinate System to Projected Coordinates > Continental > North America > North America Lambert Conformal Conic. Once the projection was complete, that shapefile was added as a layer to my data frame.

3.2 Georeferencing Figures

The next item on the agenda involved georeferencing the figures from Harrison (1972) and Cressman (1989). To do this, I selected Add Data and found the associated .tiff. I changed the frame to the layer of interest using the drop-down menu next to Georeferencing, zoomed to the area of interest and selected Fit To Display. I also changed the transparency of my figure to 50% and began georeferencing available landmarks. When applicable, I added a control point, right clicked on that control point, selected Input DMS on Lon and Lat and entered in the necessary degrees, minutes, and seconds for greater accuracy. All other instances incorporated georeferencing figures using the intersections of state lines.

This was the general work flow for georeferencing .tiffs from Harrison (1972). However, the greatest hurdle came from illustrations by Cressman (1989) because they were on a palinspastic base. This means measured sections have been restored to their proposed original location before Laramide-Sevier deformation and translation approximately 150 km to the northeast. This posed

a problem because their features of interest plotted outside current outcrop extents for the Belt-Purcell basin, which is where the isopach and paleocurrent information were plotted by Harrison (1972) making it difficult to make comparisons between both analyses. Therefore, I overcame this obstacle by georeferencing the figure which contained the palinspastic restoration in relation to the modern location of their measured sections by inputting the DMS on Lon and Lat as well as state lines. Then, I essentially unrestored Cressman's restoration by georeferencing the figures containing the isopach and paleocurrent data using control points which tied all available measured sections to their current location (fig. 1).

3.3. Generating a Geodatabase

This project involved a fair bit of heads-up digitizing which meant I needed a Geodatabase and a Feature Dataset. This was accomplished by opening ArcCatalog within ArcMaps and finding the folder within my flash drive where I have been working and saving my data. I right clicked on that folder > New > File Geodatabase. I then right clicked on my new Geodatabase and selected New > Feature Dataset.

3.3. Digitizing Lines

To digitize the isopachs, I generated a new feature class for each figure making it easier to zoom-to or hide different layers. This was done by right clicking on my Feature Dataset > New > Feature Class. The Type was changed to Line Features and the Configuration Keyword was set to Default. Various Field Names with their Data Type and Default Values were included (table 2). Including a Default Value is not necessary; however, incorporating this step will increase the efficiency and accuracy of capturing the correct information while digitizing by eliminating the post-processing step of including this data after the fact. Once my feature class was created, I selected Editor >

Start Editing > Layer of Interest > OK. Then, within the editing toolbar, I clicked on Create Features. This will open a Create Features window where I once again selected the layer of interest and selected Line in the Construction Tools below. After I traced a particular isopach, I right clicked on the last vertex and selected Finish Sketch. From there, I entered the contour interval in the Attributes window and, if necessary, changed the Confidence from Certain to Inferred (fig. 2). Once all desired features were captured, I selected Save Edits and Stop Editing. The lines types were changed within the Symbology tab of the Layer Properties window using Categories > Unique Values > Confidence > Add All Values. A solid line was chosen where the Confidence is Certain and dashed where the Confidence is Inferred. I then proceeded to repeat these steps for all georeferenced figures with applicable isopach information (fig. 4, 5, 6, 7, 8, 9 and 10).

3.4. Digitizing Points

When it came to digitizing the paleocurrents, I also created a feature class for each figure. This was accomplished by right clicking on my Feature Dataset within my Geodatabase and selecting New > Feature Class. The Type was set to Point Features and the Keyword Configuration was set to Default. Numerous Field Names, Data Types and Default Values were also included (table 3). Once my feature class was generated, I found the layer I wanted to edit in the Table of Contents, right clicked and selected Edit Feature > Start Editing. Within my editing toolbar I clicked on Create Features. This opened the Create Features window where I selected the layer of interest as well as Point within the Construction Tools. I then proceeded to add a new point for all paleocurrents. The next step involved changing the point type in the Symbology tab of the Layer Properties window and choosing Features > Single Symbol. I then changed the symbol to Flow Direction from the Style Reference called Geology 24K and set the angle to 90. This was followed by selecting Advanced > Rotation > Azimuth and Geographic. These steps are critical and must

be completed in sequence because each task sets up the next step in the process. This method is beneficial for generating paleocurrent points with a default azimuth that points north. From there, all that was required was rotating the already added points using the Rotate tool in the Editor toolbar to their respective azimuths indicated by the georeferenced figure (fig. 3) which also populated the Attribute Table. Once finished, I selected Save Edits and Stop Editing, and repeated these steps for all images that contained a sufficient amount of paleocurrent directions (fig. 5 and 6)

4. ArcGIS PROCESSING

4.1. Provenance Quantification in ArcGIS

To test whether sediment source regions for the Belt-Purcell Basin have a paleocurrent component originating from the mystery western craton, I decided to use ArcGIS to calculate the average paleocurrent direction for each figure containing digitized points. However, the only two figures I decided had a considerable amount of paleocurrents worth digitizing for this project was figure 38 and 39 from Cressman (1989). These both depict Member G and H of the Prichard Formation in the Lower Belt of the Belt-Purcell Supergroup. I accomplished this by right clicking on the feature class of interest and selecting Open Attribute Table. Within the now open Table, I right clicked on the Field Name titled Azimuth and chose Statistics (fig. 11 and 12).

4.2. Provenance Results in ArcGIS

Statistics calculated for the azimuth of Member G in the Prichard Formation using ArcMaps shows a count of 33, a minimum and maximum azimuth of 1° and 354° respectively, as well as a mean value of 124° (fig. 11). On the other hand, statistics for Member H of the Prichard Formation

illustrate a count of 12, a calculated minimum of 26° and maximum of 359° , in addition to a mean of 198° (fig. 12).

However, there is a glaring problem with the Statistics calculation of the mean azimuth using ArcGIS. This is most notable for Member H of the Prichard Formation, where the Frequency Distribution generally shows a paleoflow direction to the northwest, north, and northeast (fig. 12). However, ArcGIS calculated a mean paleoflow toward the south-southwest, so this statistic calculation is fundamentally flawed and the same must be true for the calculations from Member G of the Prichard Formation (fig. 11).

5. EXCEL PROCESSING

5.2. Provenance Quantification in Excel

Therefore, a new calculation had to be made. This was accomplished in Excel, and since I had already captured the necessary azimuthal values when the paleocurrents were digitized, the calculation was straightforward. This was accomplished by opening the Attribute Table for the layer of interest in ArcMaps, selecting each row that contains a paleocurrent, right clicking and selecting Copy Selected. I then pasted this information in Excel, converted the azimuthal values from degrees to radians, took the sine and cosine for the radians of each azimuth, summed up the sines and cosines, then calculated the arctangent of the sum of the sines divided by the sum of the cosines in radians, and converted this back to degrees. I made these calculations for both Member G and H of the Prichard Formation (table 4 and 5).

5.3. Provenance Results in Excel

Therefore, the results determined using excel for Member G of the Prichard Formation, which is stratigraphically lower and presumably older, shows an average paleocurrent direction toward the north (20°; table 4). This calculation is supported by observations from the isopach map (fig. 5). Based on thickness trends, current directions, and lithologies interpreted as turbidites deposited in a submarine fan, Member G is what Cressman (1989) refers to as the Prichard fan with sediment provenance from a non-Laurentian southern source.

On the other hand, the average azimuth calculated in Excel for Member H of the Prichard Formation is also toward the north (017°; table 5); however, the isopach map (fig. 6) has a vastly different morphological expression from Member G. According to Cressman (1989), Member H has also been interpreted as turbidite deposits with sediment provenance from the non-Laurentian craton to the south, with the only difference being that these deposited marginal to the Prichard fan.

6. DISCUSSION & CONCLUSION

In all honesty, even though the average paleocurrent directions imply a non-Laurentian southern sediment provenance source, results presented herein only comprise the Prichard Formation in the Lower Belt. This means my hypothesis for the entire Belt-Purcell Supergroup remains unresolved. With regards to the progress completed on my project thus far, I was fortunate enough to be able to digitize numerous isopach maps (fig. 4, 5, 6, 7, 8, 9 and 10). Needless to say, my hope was to find more paleocurrent information that would support trends observed in the isopach contours. However, these methods detailed herein generated from the two figures that contained sufficient paleocurrent information from Cressman (1989), arguably serve as a proof-of-concept. And even though the average paleocurrent calculations were completed in

Excel, testing this hypothesis necessitated ArcMaps to restore the features from Cressman within current Belt-Purcell basin outcrops for comparison with work by Harrison (1972), and to generate the azimuthal values for paleocurrents by Cressman (1989) since the data tables are unpublished.

When it comes to the consideration of caveats, confounding factors, and limiting assumptions, numerous examples come to mind. First, a small margin of error was no doubt created while georeferencing figures, palinspastically unrestored or otherwise. This uncertainty was likely inflated by the distortion generated when I unrestored the palinspastic sections to their modern locations within the boundary of the Belt-Purcell Supergroup. Additionally, the azimuths created while digitizing point features likely contain an uncertainty of plus or minus a few degrees. And finally, calculating the average of all paleocurrents available for a particular stratigraphic unit is obviously an oversimplification; however, the overall regional trends are beneficial, but not a be-all end-all, with regards to sediment provenance analyses.

Regardless, I intend to expand this dataset with published work from other researchers, in addition to measured sections and paleocurrent information I hope to collect this summer with a field assistant. To date, there are no published paleoflow directions for any stratigraphic units above the Bonner Formation in the Missoula Group, generating the need for more data. These results will have important implications for tectonic reconstructions of the Mesoproterozoic supercontinent Columbia.

REFERENCES

- Cressman, E.R., 1989, Reconnaissance stratigraphy of the Prichard Formation (middle Proterozoic) and the early development of the Belt Basin, Washington, Idaho, and Montana: Professional Paper, doi:10.3133/pp1490.
- Harrison, J.E., 1972, Precambrian Belt Basin of Northwestern United States: Its Geometry, Sedimentation, and Copper Occurrences: GSA Bulletin, v. 83, p. 1215–1240, doi:10.1130/0016-7606(1972)83[1215:PBBONU]2.0.CO;2.
- McKenzie, D., Daly, M.C., and Priestley, K., 2015, The lithospheric structure of Pangea: Geology, v. 43, p. 783–786, doi:10.1130/G36819.1.
- Meert, J.G., and Santosh, M., 2017, The Columbia supercontinent revisited: Gondwana Research, v. 50, p. 67–83, doi:10.1016/j.gr.2017.04.011.
- Meert, J.G., and Torsvik, T.H., 2003, The making and unmaking of a supercontinent: Rodinia revisited: Tectonophysics, v. 375, p. 261–288, doi:10.1016/S0040-1951(03)00342-1.
- Puetz, S.J., 2018, A relational database of global U–Pb ages: Geoscience Frontiers, v. 9, p. 877–891, doi:10.1016/j.gsf.2017.12.004.

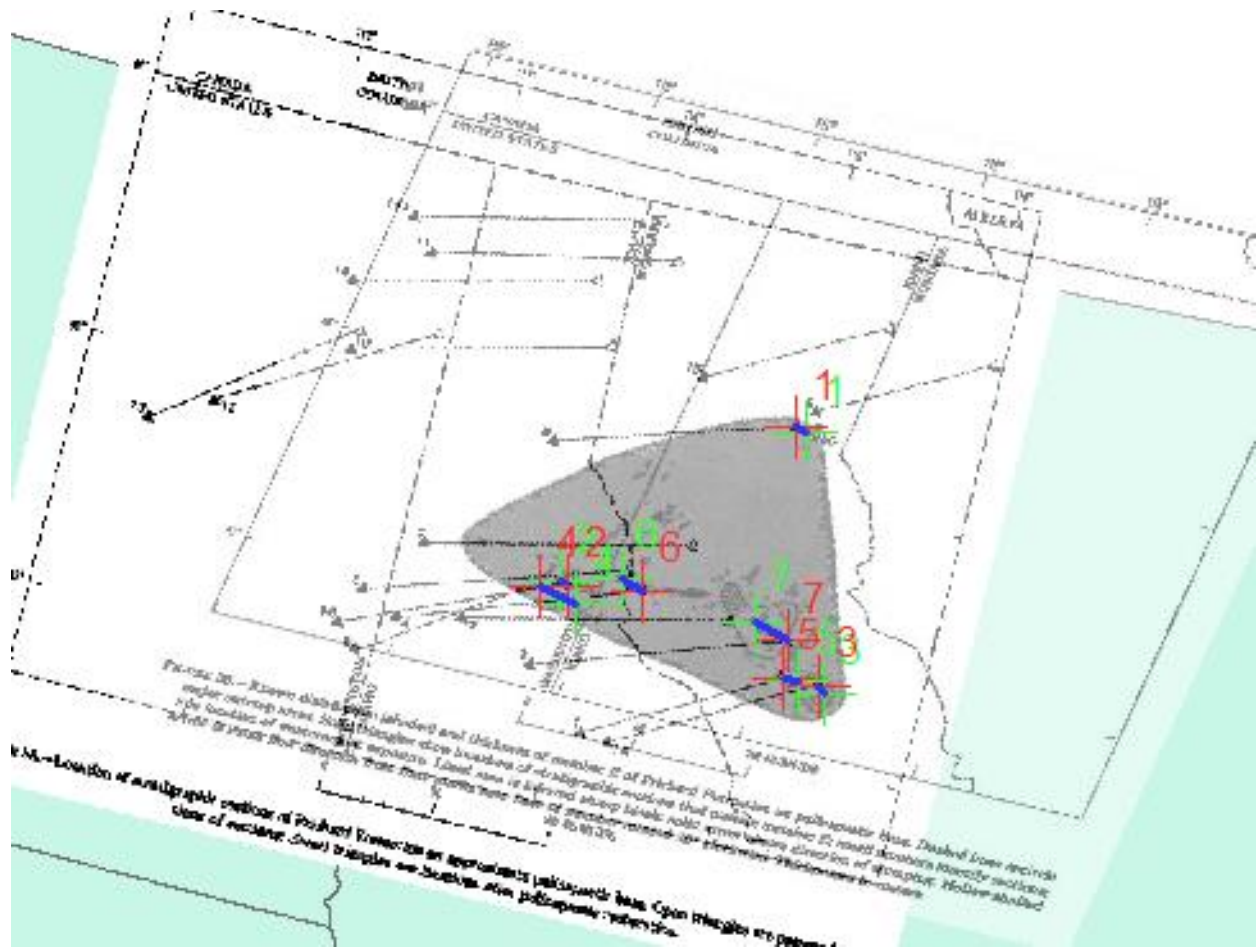


Figure 1. Screen grab of ArcMaps highlighting my process of georeferencing figures. This example shows the US state boundaries (blue fill color), the georeferenced image indicating the modern location of measured sections and their palinospastic restorations (left), and a figure from Cressman (1989) that is being georeferenced (right). This particular .tiff demonstrates the location of 7 palinospastically restored sections; therefore, 7 control points (red and green plus symbols) were used to unrestore these sections to their modern positions.

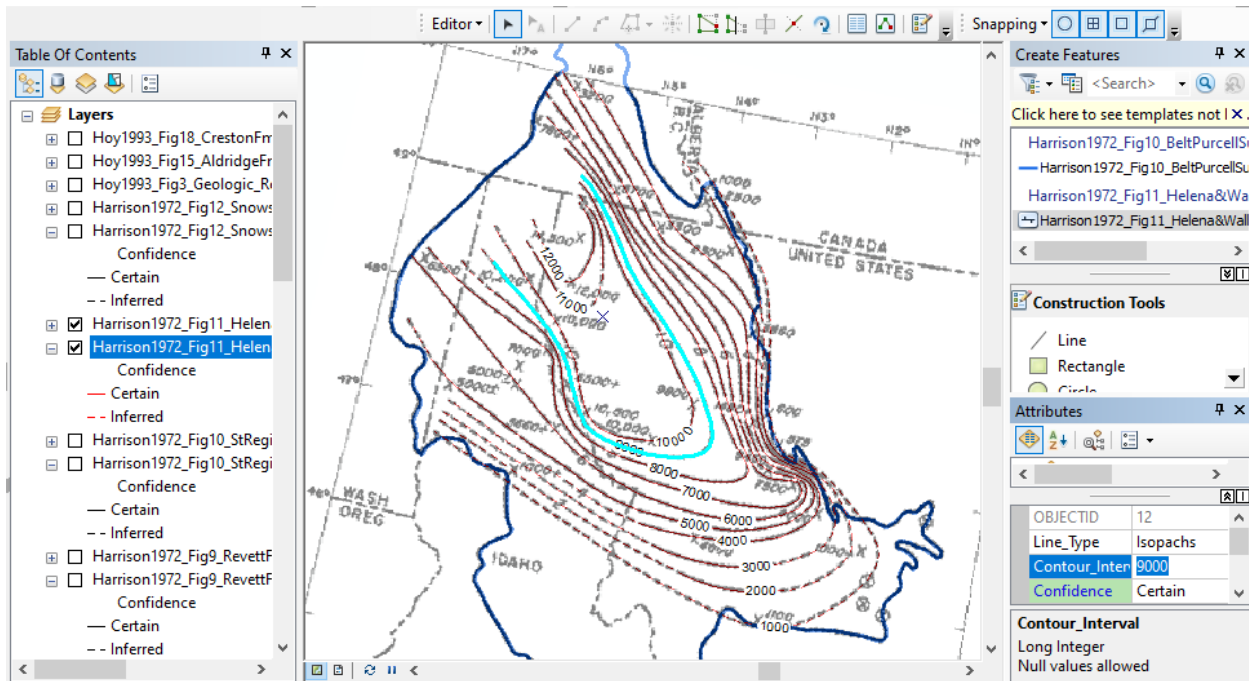


Figure 2. Screen capture of ArcMaps illustrating my workflow through digitizing isopach maps as line features. This is an example of the 9000 ft contour interval from the Helena, Wallace, and Kitchener Formations in figure 11 from Harrison (1972).

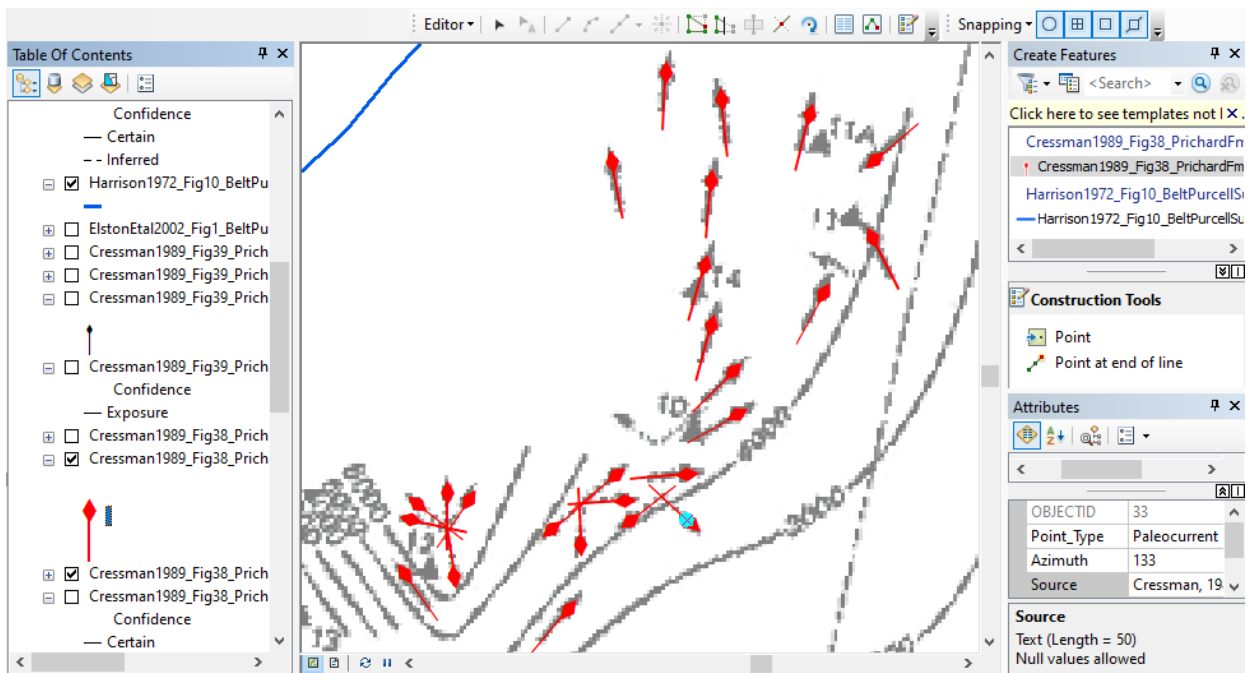


Figure 3. Screen grab of ArcMaps demonstrating my workflow through digitizing paleocurrents as points. An example is shown here from Member G of the Prichard Formation in figure 38 of Cressman (1989).

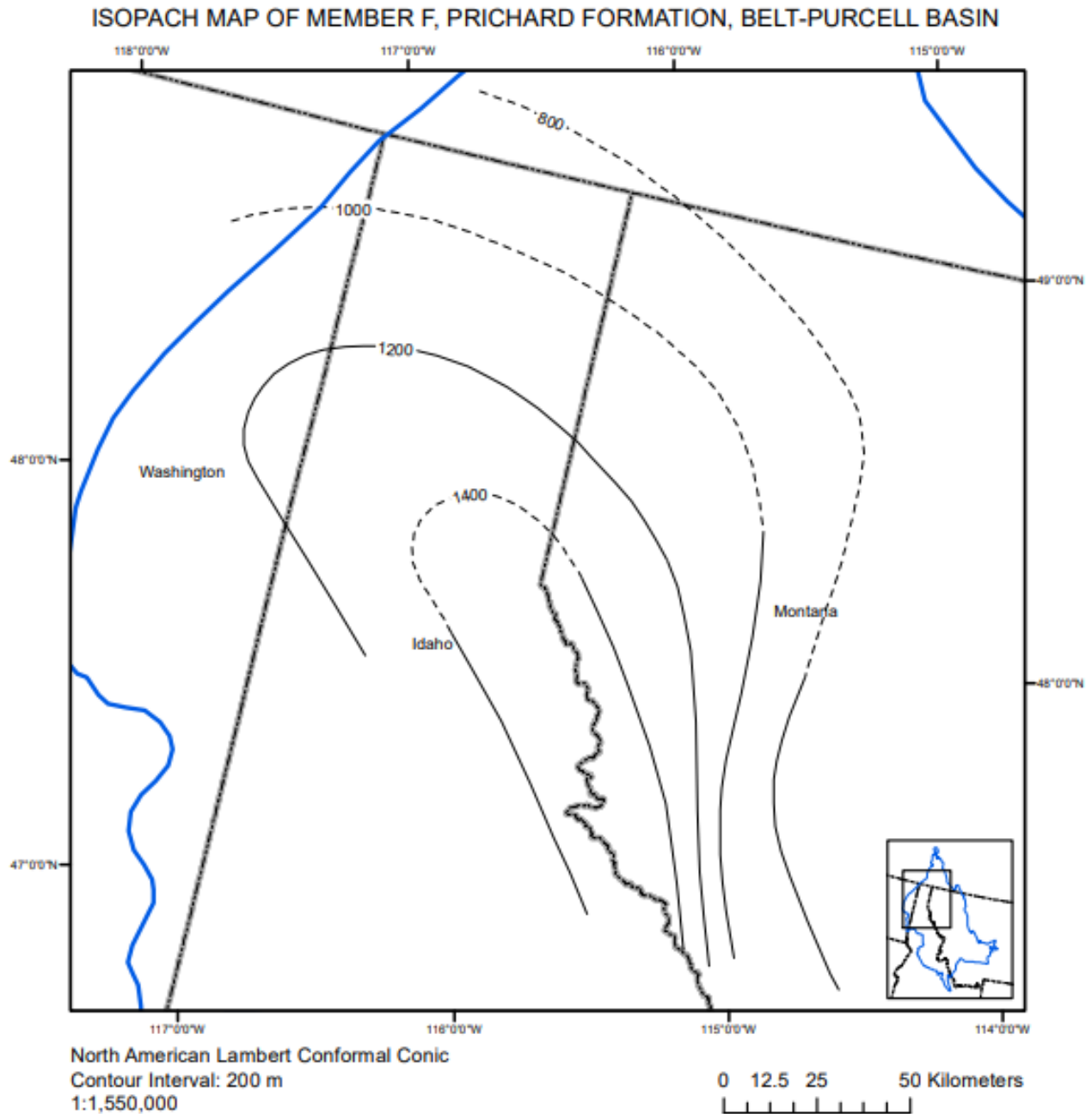


Figure 4. Isopach map of Member F of the Prichard Formation in the Belt-Purcell basin. Certain (solid black lines) and inferred (dashed black lines) isopachs are illustrated with their contour intervals (black numbers); meanwhile, the current outcrop extent for the Belt-Purcell Supergroup (solid blue line) and US state boundaries (grey and black dashed line) are also depicted. This information was collected from figure 37 of Cressman (1989).

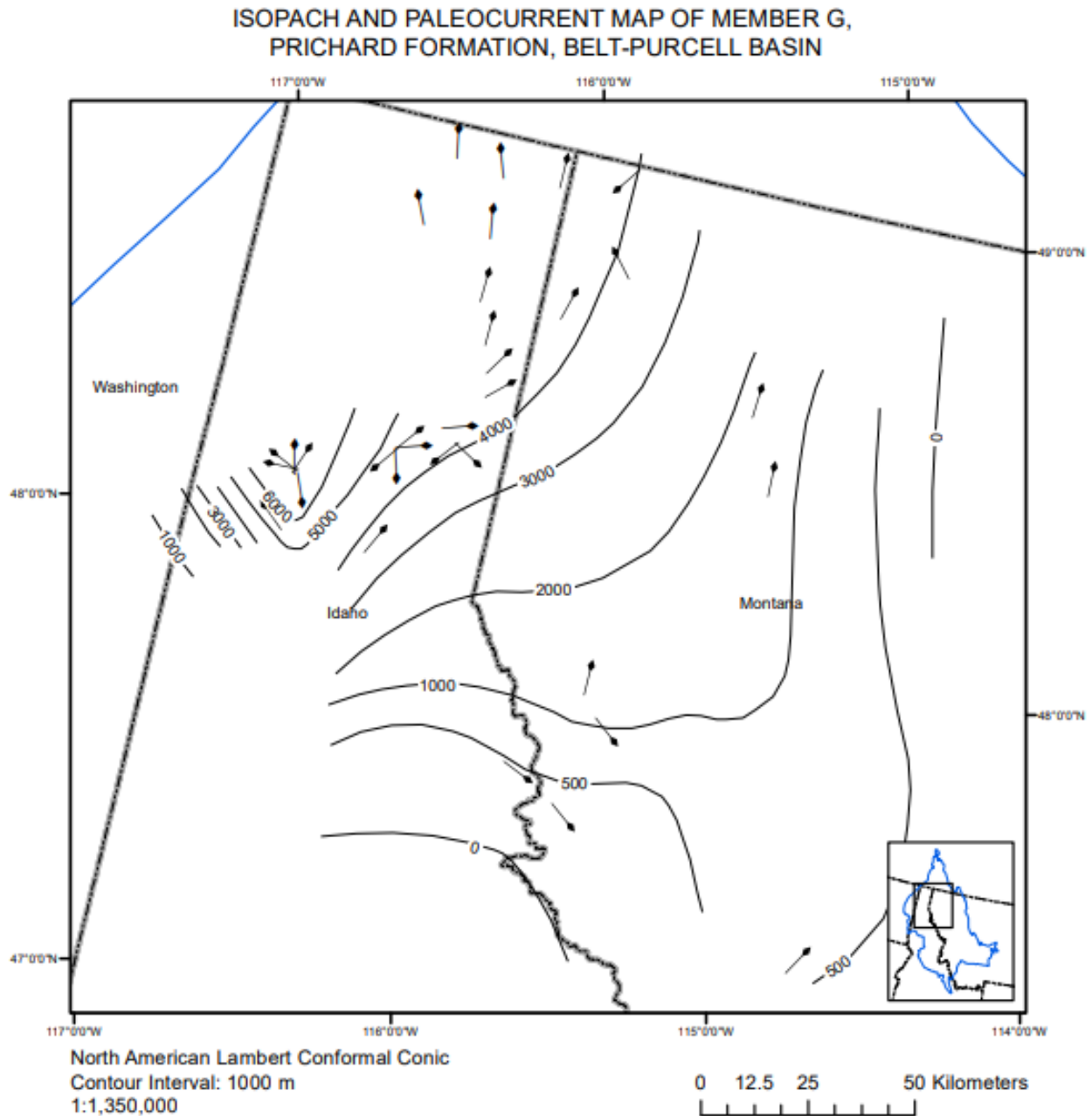


Figure 5. Isopach and paleocurrent map of Member G of the Prichard Formation in the Lower Belt of the Belt-Purcell basin. Certain (solid black lines) and inferred (dashed black lines) isopachs are illustrated with their contour intervals (black numbers) along with the paleocurrents (flow direction symbol; tail indicates source region); meanwhile, the current outcrop extent for the Belt-Purcell basin (solid blue line) and US state boundaries (grey and black dashed line) are also indicated. This data was generated from figure 38 of Cressman (1989).

ISOPACH AND PALEOCURRENT MAP OF MEMBER H,
PRICHARD FORMATION, BELT-PURCELL BASIN

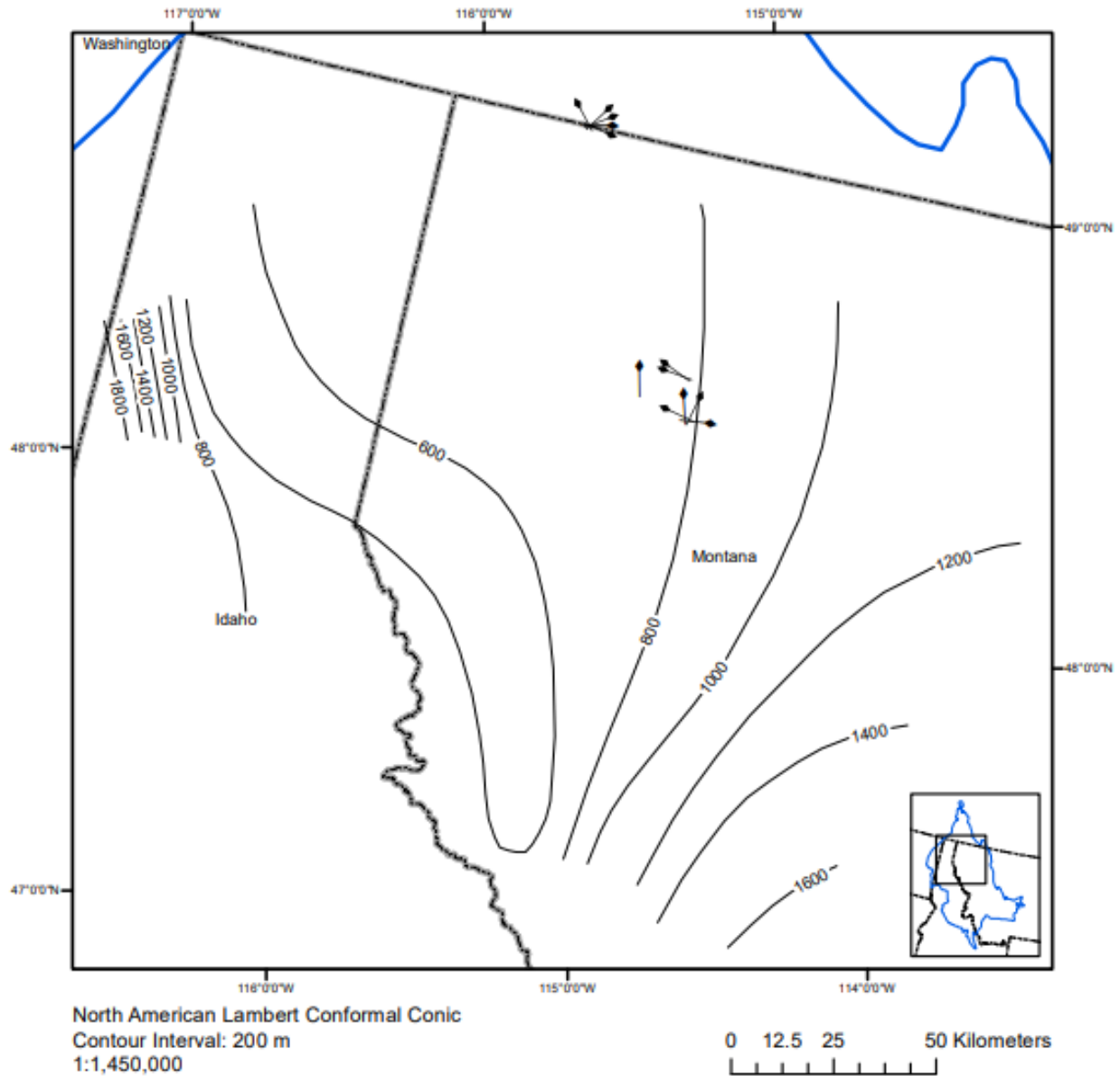


Figure 6. Isopach and paleocurrent map of Member H of the Prichard Formation in the Belt-Purcell Supergroup. Certain (solid black lines) and inferred (dashed black lines) isopachs are illustrated with their contour intervals (black numbers) and paleocurrents (flow direction symbol; head indicates flow direction); meanwhile, the current outcrop extent for the Belt-Purcell basin (solid blue line) and US state boundaries (grey and black dashed line) are also depicted. This information was compiled from figure 39 of Cressman (1989).

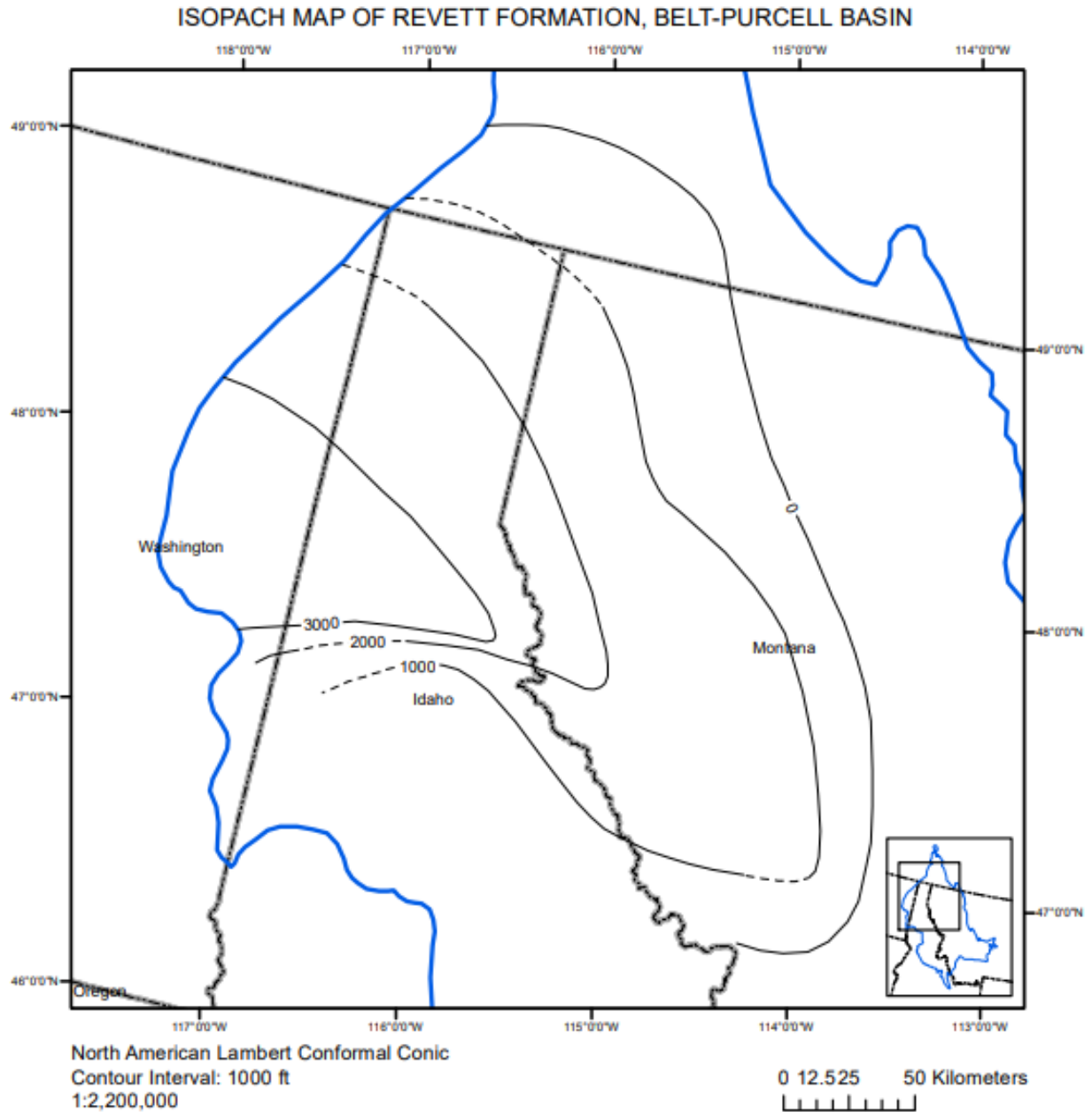


Figure 7. Isopach map of the Revett Formation from the middle portion of the Ravalli Group in the Belt-Purcell basin. Certain (solid black lines) and inferred (dashed black lines) isopachs were digitized with their contour intervals (black numbers); meanwhile, the current outcrop extent for the Belt-Purcell Supergroup (solid blue line) and US state boundaries (grey and black dashed line) are also illustrated. This information was collected from figure 9 of Harrison (1972).

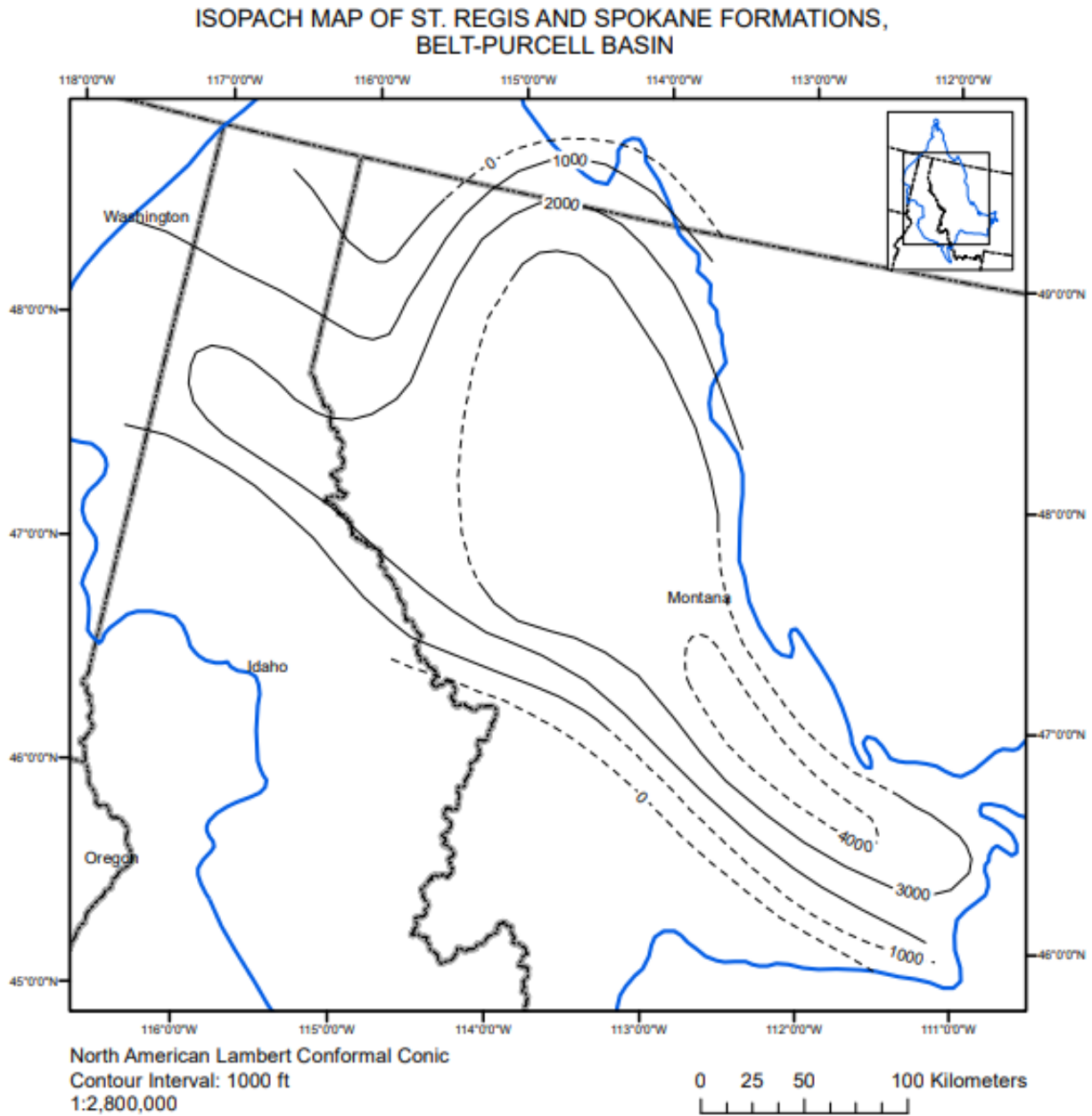


Figure 8. Isopach map of the St. Regis and Spokane formations from the upper portion of the Ravalli Group in the Belt-Purcell basin. Certain (solid black lines) and inferred (dashed black lines) isopachs are illustrated with their contour intervals (black numbers); meanwhile, the current outcrop boundary for the Belt-Purcell Supergroup (solid blue line) and US state lines (grey and black dashed line) are also depicted. This information was compiled from figure 10 of Harrison (1972).

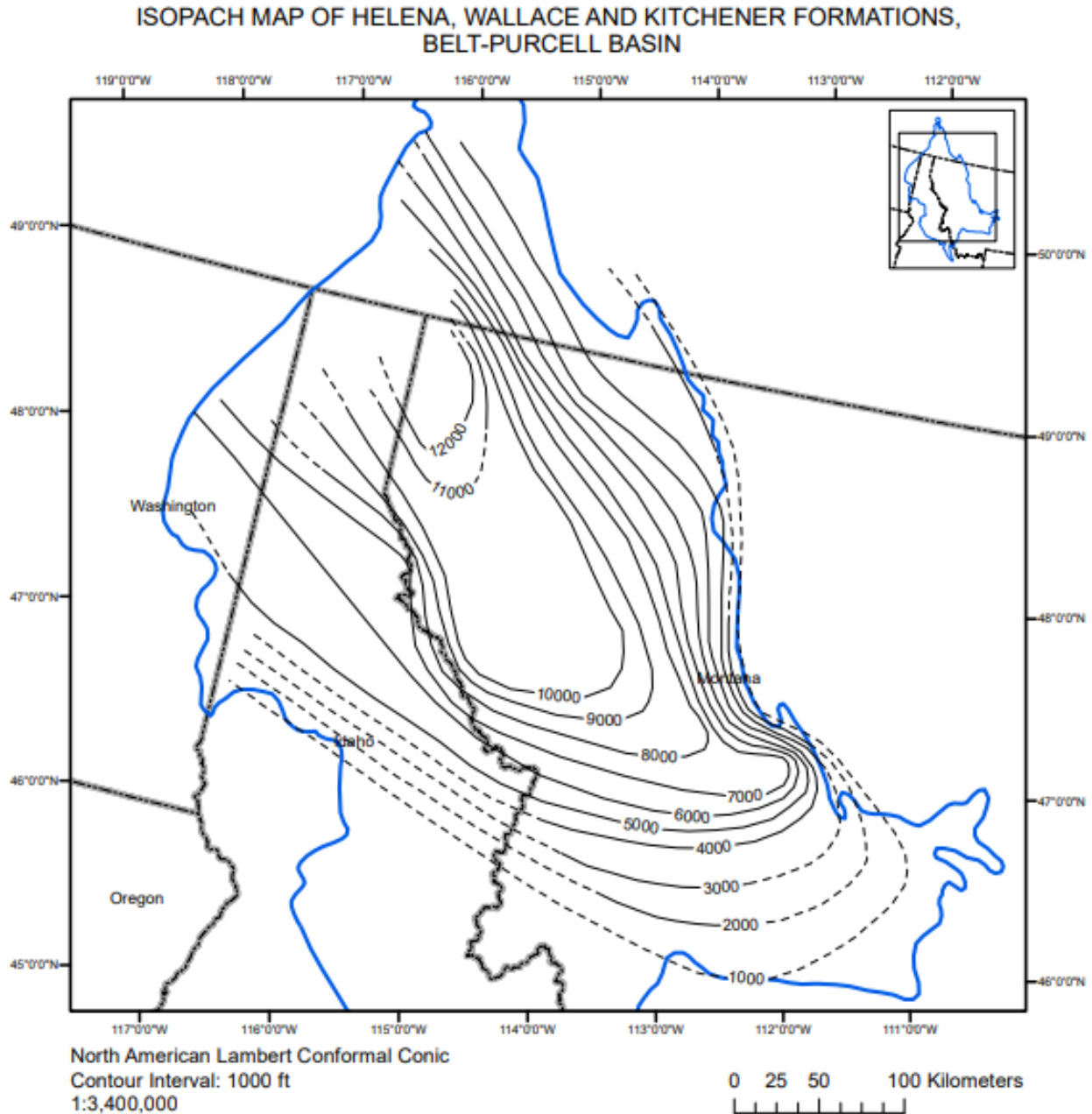


Figure 9. Isopach map of the Helena, Wallace and Kitchener Formations of the Middle Belt carbonate in the Belt-Purcell Supergroup. Certain (solid black lines) and inferred (dashed black lines) isopachs are demonstrated with their contour intervals (black numbers); meanwhile, the current outcrop extent for the Belt-Purcell basin (solid blue line) and US state boundaries (grey and black dashed line) are also depicted. This information was generated from figure 11 of Harrison (1972).

ISOPACH MAP OF SNOWSLIP, SHEPPARD, MT. SHIELDS AND BONNER FORMATION,
BELT-PURCELL BASIN

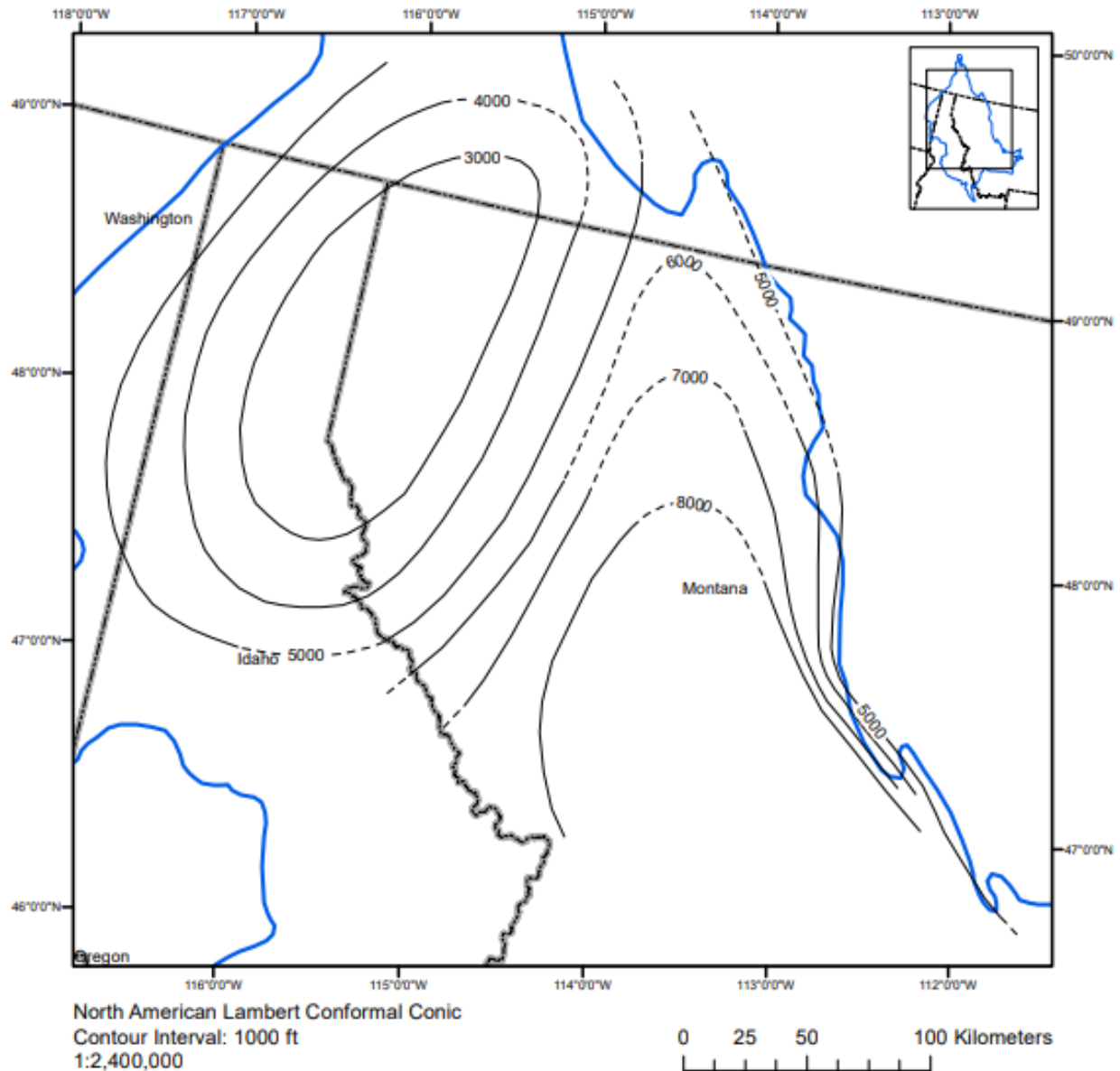


Figure 10. Isopach map of the Snowslip, Sheppard, Mt. Shields and Bonner Formations of the Missoula Group in the Belt-Purcell basin. Certain (solid black lines) and inferred (dashed black lines) isopachs are illustrated with their contour intervals (black numbers); meanwhile, the current outcrop boundary for the Belt-Purcell Supergroup (solid blue line) and US state boundaries (grey and black dashed line) are also demonstrated. This information was generated from figure 12 of Harrison (1972).

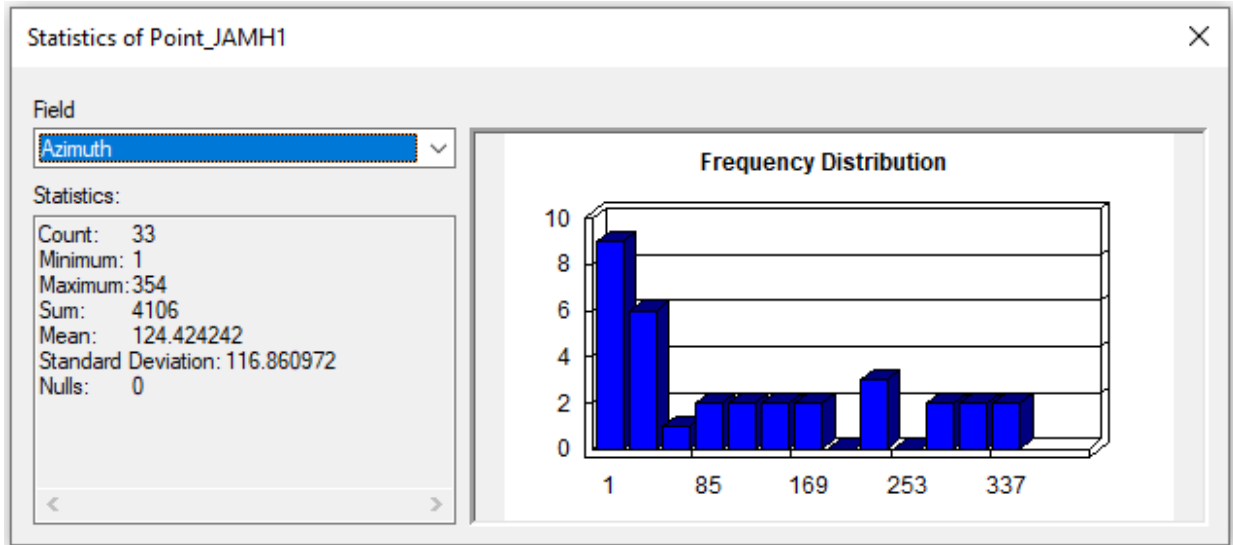


Figure 11. Results for the Azimuth field using Statistics from the Attribute Table. This data depicts Member G from the Prichard Formation of the Belt-Purcell basin from figure 38 of Cressman (1989).

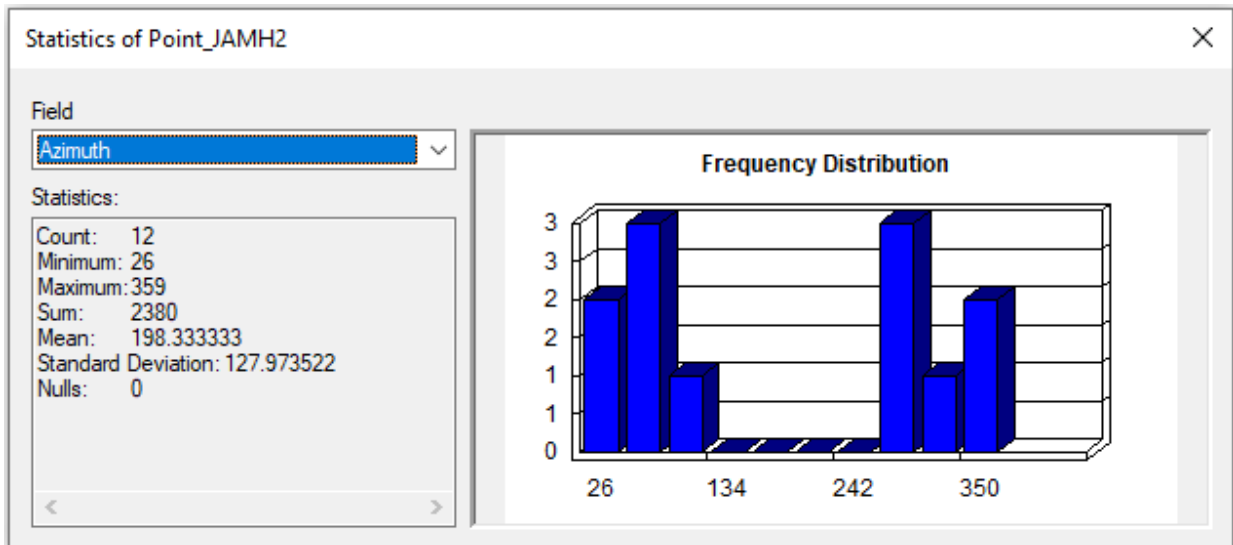


Figure 12. Results for the Statistics of the Azimuths field from Member H of the Prichard Formation of the Lower Belt in the Belt-Purcell Supergroup from figure 39 of Cressman (1989).

Source	Figure	Feature Represented	URL	Spatial Reference	File Type
USGS	n/a	US State Boundary	https://www.sciencebase.gov/catalog/item/5eaa545982cefae35a22231f	NAD83	.shp
Harris on, 1972	12	Isopachs of Snowslip, Sheppard, Mt. Shields and Bonner Fm	https://pubs-geoscienceworld-org.ezproxy.lib.utexas.edu/gsa/gsabulletin/article/83/5/1215/7523/P-recambrian-Belt-Basin-of-Northwestern-United?searchresult=1	Unknown	.tiff
Harris on, 1972	11	Isopachs of Helena, Wallace and Kitchener Fm	https://pubs-geoscienceworld-org.ezproxy.lib.utexas.edu/gsa/gsabulletin/article/83/5/1215/7523/P-recambrian-Belt-Basin-of-Northwestern-United?searchresult=1	Unknown	.tiff
Harris on, 1972	10	Isopachs of St. Regis and Spokane Fm	https://pubs-geoscienceworld-org.ezproxy.lib.utexas.edu/gsa/gsabulletin/article/83/5/1215/7523/P-recambrian-Belt-Basin-of-Northwestern-United?searchresult=1	Unknown	.tiff
Harris on, 1972	9	Isopachs of Revett Fm	https://pubs-geoscienceworld-org.ezproxy.lib.utexas.edu/gsa/gsabulletin/article/83/5/1215/7523/P-recambrian-Belt-Basin-of-Northwestern-United?searchresult=1	Unknown	.tiff
Harris on, 1972	9	Belt-Purcell Boundary	https://pubs-geoscienceworld-org.ezproxy.lib.utexas.edu/gsa/gsabulletin/article/83/5/1215/7523/P-recambrian-Belt-Basin-of-Northwestern-United?searchresult=1	Unknown	.tiff
Cress man, 1989	39	Isopachs and Paleocurrents of Prichard Fm, Member H	https://pubs.er.usgs.gov/publication/pp1490	Unknown	.tiff
Cress man, 1989	38	Isopachs and Paleocurrents of Prichard Fm, Member G	https://pubs.er.usgs.gov/publication/pp1490	Unknown	.tiff
Cress man, 1989	37	Isopachs of Prichard Fm, Member F	https://pubs.er.usgs.gov/publication/pp1490	Unknown	.tiff

Table 1. Compiled list of data collected for this study indicating the source, figure number, particular feature captured, its spatial reference, file type and their associated websites. Stratigraphic formations are listed in order with oldest to youngest being bottom to top.

Field Name	Data Type	Default Value
Line_Type	Text	Isopach
Contour_Interval	Long Integer	<null>
Confidence	Text	Certain
Source	Text	Harrison, 1972
Figure	Long Integer	11
Unit_Name	Text	Helena, Wallace and Kitchener Formations

Table 2. List of information incorporated when creating new feature class for line features. This is an example for the Helena, Wallace, and Kitchener formations of figure 11 from Harrison (1972).

Field Name	Data Type	Default Value
Line_Type	Text	Paleocurrent
Azimuth	Long Integer	<null>
Source	Text	Cressman, 1989
Figure	Long Integer	38
Unit_Name	Text	Prichard Formation, Member G

Table 3. Compilation of Field Names, Data Types and Default Values included when creating feature classes to digitize paleocurrents as points. The example shown here is for Member G of the Prichard Formation from figure 38 from Cressman (1989).

azi deg	azi rad	sin(azi rad)	cos(azi rad)
349	6.091199089	-0.190808995	0.981627183
17	0.296705973	0.292371705	0.956304756
85	1.483529864	0.996194698	0.087155743
61	1.064650844	0.874619707	0.48480962
46	0.802851456	0.7193398	0.69465837
15	0.261799388	0.258819045	0.965925826
40	0.698131701	0.64278761	0.766044443
325	5.672320069	-0.573576436	0.819152044
29	0.506145483	0.48480962	0.874619707
333	5.811946409	-0.4539905	0.891006524
229	3.996803987	-0.75470958	-0.656059029
14	0.244346095	0.241921896	0.970295726
354	6.178465552	-0.104528463	0.994521895
3	0.052359878	0.052335956	0.998629535
5	0.087266463	0.087155743	0.996194698
16	0.27925268	0.275637356	0.961261696
12	0.20943951	0.207911691	0.978147601
14	0.244346095	0.241921896	0.970295726
142	2.478367538	0.615661475	-0.788010754
127	2.21656815	0.79863551	-0.601815023
141	2.460914245	0.629320391	-0.777145961
44	0.034906585	0.034899497	0.999390827
282	4.921828491	-0.978147601	0.207911691
308	5.375614096	-0.788010754	0.615661475
1	0.017453293	0.017452406	0.999847695
34	0.593411946	0.559192903	0.829037573
171	2.984513021	0.156434465	-0.987688341
230	4.01425728	-0.766044443	-0.64278761
177	3.089232776	0.052335956	-0.998629535
86	1.500983157	0.99756405	0.069756474
51	0.890117919	0.777145961	0.629320391
232	4.049163865	-0.788010754	-0.615661475
133	2.321287905	0.731353702	-0.68199836

sum(sin)	sum(cos)
4.616641812	12.67377949

atan(sumsin/sumcos)	degree(atan)
0.349328028	20.01502166

Table 4. Results for the average paleocurrent direction for Member G of the Prichard Formation in the Lower Bet of the Belt-Purcell Supergroup. Azimuths were generated from figure 38 of Cressman (1989) using ArcMaps with these equations being calculated in Excel.

azi deg	azi rad	sin(azi rad)	cos(azi rad)
359	6.265732015	-0.017452406	0.999847695
290	5.061454831	-0.939692621	0.342020143
306	5.340707511	-0.809016994	0.587785252
295	5.148721293	-0.906307787	0.422618262
356	6.213372137	-0.069756474	0.99756405
26	0.453785606	0.438371147	0.898794046
96	1.675516082	0.994521895	-0.104528463
332	5.794493117	-0.469471563	0.882947593
47	0.820304748	0.731353702	0.68199836
69	1.204277184	0.933580426	0.35836795
90	1.570796327	1	6.12574E-17
114	1.989675347	0.913545458	-0.406736643

sum(sin)	sum(cos)
1.799674783	5.660678245

atan(sumsin/sumcos)	degree(atan)
0.307820141	17.63679495

Table 5. Results for the average paleocurrent direction for Member H of the Prichard Formation in the Lower Bet of the Belt-Purcell Supergroup. Azimuths were generated from figure 39 of Cressman (1989) using ArcMaps with these equations being calculated in Excel.